Compact Circular Sector and Annular Sector Dielectric Resonator Antennas

Matthew T. K. Tam and Ross D. Murch, *Senior Member, IEEE*

***Abstract*— In this paper, we investigate circular sector and annular sector dielectric resonator antenna (DRA) geometries. The advantage these geometries offer, compared to conventional circular cylindrical DRA's, are significant reductions in volume, making them potential candidates for use in compact applications such as mobile communication handsets. Approximate theory, simulation, and experimental results are provided to support our findings. In particular, a sector DRA is demonstrated to have 75% less volume than a conventional cylindrical DRA, with the same resonant frequency. DRA volume minimization for compact antenna design is also discussed and a design is proposed and tested for a mobile telephone handset suitable for the DCS1800 system.**

***Index Terms*—Dielectric resonator antennas.**

I. Introduction

RECENTLY dielectric resonators have been demonstrated to be practical elements for antenna applications and have several merits including high radiation efficiency, flexible feed arrangement, simple geometry, and compactness [1]–[3]. In this paper, we investigate circular sector and annular sector dielectric resonator antenna (DRA) geometries that are formed by removing a sector (or, equivalently, a wedge) of dielectric material from a circular or annular cylinder.

The motivation for performing this investigation is to attempt to design DRA's that are sufficiently compact for use in wireless communication handsets. DRA's can potentially be integrated into wireless communication handsets and could offer several advantages over conventional external antennas such as monopoles and helix. These advantages include being less easily broken off, reduced power absorption by the head and less sensitivity to the geometry of the handset. One of the disadvantages of DRA's for wireless communication handsets however is that they are not as compact as alternative approaches such as planar inverted F antenna (PIFA) [6]–[9] and therefore methods need to be devised to reduce the size of the DRA.

In this paper we demonstrate that significant reductions in the volume of the DRA can be obtained by utilizing circular sector and annular sector DRA's.

In Section II we review and describe approximate theory to analyze the sectored and annular DRA designs. Methods for volume minimization are discussed in Section III while FDTD simulation results are provided in Section IV. Experimental results are provided in Section V and a design suitable for a mobile telephone handset is given in Section VI.

Manuscript received May 22, 1998; revised December 9, 1998. This work was supported by the Hong Kong Research Grants Council.

The authors are with the Department of Electrical and Electronic Engineering, The Hong Kong University of Science and Technology, Kowloon, Hong Kong.

Publisher Item Identifier S 0018-926X(99)04828-0.

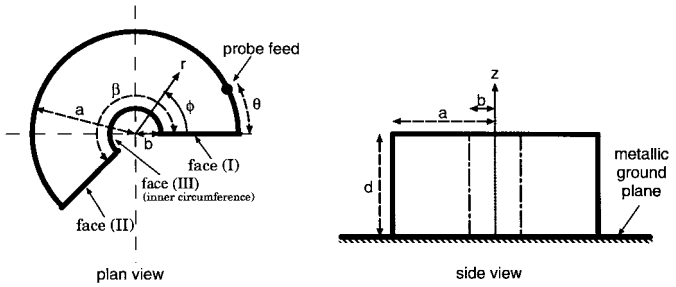

Fig. 1. General geometry of a circular or annular sector DRA. Sector faces (I) or (II) and inner circumference (III) can be metallic plates or left open.

II. Approximate Theory

The general DRA we consider is shown in Fig. 1. It consists of a circular DRA of height d and radius a, on a metallic ground plane, with a sector and circular core of dielectric material removed. The sector angle is denoted as β while b is taken as the inner radius so that the ratio defined by $\alpha = b/a$ is between zero and unity. The sector faces (I), (II), and the inner circular surface (III) can be metallized or left open. Depending on the setting of β and α, circular $(\beta = 2\pi, \alpha = 0)$, sectored $(\beta < 2\pi, \alpha = 0)$, annular $(\beta = 2\pi, \alpha > 0)$, and sectored-annular $(\beta < 2\pi, \alpha > 0)$ DRA's can be formed.

A. Cavity Model

To provide an approximate analysis of the fields inside the circular and annular sectored DRA and also predict its resonant frequency we invoke the cavity resonator model where the outer surfaces of the cavity are approximated by magnetic walls [1], [2]. The resulting solution for the field inside the DRA, in terms of the $\mathrm{TM}_{\nu pm+\delta}$ mode, is

$$E_z^{\nu pm} = [AJ_\nu(k_r r) + BY_\nu(k_r r)] \cdot [C\sin(\nu\phi) + D\cos(\nu\phi)]\cos(k_z z) \quad (1)$$

for $b \le r \le a$, $0 \le \phi \le \beta$, $0 \le z \le d$ where ν is a positive real number that depends on the boundary conditions on the sector faces as well as the sector angle while p, m are positive integers and k_r, k_z are wavenumbers. The functions J_ν, Y_ν denote the νth-order Bessel functions of the first and second kind, respectively, and the complex constants A, B, C, and D depend on the geometry and feed.

TABLE I
ROOTS OF THE CHARACTERISTIC EQUATION
$J'_\nu(X_{\nu p}) = 0$ FOR $\alpha = 0$, AND (9) FOR $\alpha > 0$

		$\nu=0$	$\nu=\frac{1}{4}$	$\nu=\frac{1}{3}$	$\nu=\frac{1}{2}$	$\nu=\frac{2}{3}$	$\nu=1$	$\nu=2$
$\alpha=0$,	$p=1$	3.832	0.769	0.910	1.166	1.401	1.841	3.054
	$p=2$	7.016	4.225	4.353	4.604	4.851	5.331	6.706
$\alpha=0.1$,	$p=1$	3.976	0.771	0.912	1.167	1.402	1.841	3.054
	$p=2$	7.342	4.280	4.397	4.633	4.869	5.339	6.707
$\alpha=0.2$,	$p=1$	4.336	0.780	0.920	1.174	1.408	1.845	3.055
	$p=2$	8.073	4.493	4.592	4.794	5.001	5.423	6.724
$\alpha=0.5$,	$p=1$	6.595	0.881	1.103	1.292	1.526	1.955	3.124
	$p=2$	12.327	6.354	6.428	6.573	6.716	7.001	7.163

TABLE II
ROOTS OF THE CHARACTERISTIC EQUATION
$J'_\nu(X_{\nu p})Y_\nu(\alpha X_{\nu p}) - J_\nu(\alpha X_{\nu p})Y'_\nu(X_{\nu p}) = 0$

		$\nu=0$	$\nu=\frac{1}{4}$	$\nu=\frac{1}{3}$	$\nu=\frac{1}{2}$	$\nu=\frac{2}{3}$	$\nu=1$	$\nu=2$
$\alpha=0$,	$p=1$	0.930*	0.769	0.910	1.166	1.401	1.841	3.054
	$p=2$	4.635*	4.225	4.353	4.604	4.851	5.331	6.706
$\alpha=0.1$,	$p=1$	1.103	1.171	1.221	1.352	1.512	1.879	3.056
	$p=2$	4.979	5.017	5.046	5.128	5.239	5.532	6.724
$\alpha=0.2$,	$p=1$	1.412	1.456	1.489	1.581	1.699	1.993	3.073
	$p=2$	5.696	5.718	5.735	5.783	5.849	6.033	6.910
$\alpha=0.5$,	$p=1$	2.722	2.738	2.751	2.786	2.836	2.973	3.619
	$p=2$	9.292	9.298	9.303	9.318	9.338	9.394	9.696

The resonant frequency of a mode $f_{\nu pm}$ is given as [1]–[2]

$$f_{\nu pm} = \frac{c}{2\pi\sqrt{\epsilon_r}}\sqrt{k_r^2 + k_z^2} = \frac{c}{2\pi a\sqrt{\epsilon_r}}\sqrt{X_{\nu p}^2 + \left[\frac{\pi a}{2d}(2m+1)\right]^2} \quad (2)$$

where c is the velocity of light in free space and the wavenumbers are as $k_r = \frac{X_{\nu p}}{a}$, $k_z = \frac{(2m+1)\pi}{2d}$, and $X_{\nu p}$ is the root satisfying the characteristic equation (see following sections).

B. Conventional Circular DRA

A conventional circular DRA is formed when $\beta = 2\pi$, $\alpha = 0$ (the faces (I), (II), and (III) are not present) and has been well investigated [1], [2]. For this geometry $\nu = n$ where n is an integer, $B = 0$ in (1) and the characteristic equation for the root $X_{\nu p}$ in (2) is

$$J'_\nu(X_{\nu p}) = 0. \quad (3)$$

Table I lists some values of $X_{\nu p}$ in which integer values of ν and $\alpha = 0$ are for this geometry.

C. Circular Sector DRA

Circular sector DRA's are formed by setting $0 < \beta < 2\pi$ and $\alpha = 0$ and, to our knowledge, have not been reported elsewhere. Three combinations for the sector faces (I) and (II) are possible and these include both metallic ($E_z|_{\phi=0} = 0$ and $E_z|_{\phi=\beta} = 0$), both open $\frac{\partial E_z}{\partial \phi}|_{\phi=0} = 0$ and $\frac{\partial E_z}{\partial \phi}|_{\phi=\beta} = 0$, or one metallic and one open face $E_z|_{\phi=0} = 0$ and $\frac{\partial E_z}{\partial \phi}|_{\phi=\beta} = 0$. The solution for the field when both faces are metallic, requires $D = 0$ in (1) and

$$\nu = \frac{n\pi}{\beta}, \qquad \text{where } 0 < \beta \le 2\pi \quad (4)$$

where n is a nonzero positive integer to satisfy the boundary conditions at face (I) and (II), respectively [10]. Similar reasoning reveals that the solution when both faces are open requires $C = 0$ and (4). When face (I) is metallic and face (II) is open the field satisfying the boundary conditions requires $D = 0$ in (1) and

$$\nu = \frac{\pi}{2\beta}(2n-1), \qquad \text{where } 0 < \beta < 2\pi. \quad (5)$$

The characteristic equation for all three configurations are the same as in (3) except that ν can now be positive real valued. Table I lists some values of $X_{\nu p}$ for different nonzero real values of ν in which $\alpha = 0$ is for these geometries.

Note the resonant frequency for a given DRA with radius a and height d depends only on $X_{\nu p}$ through the variable ν. From Table I we observe that the smaller ν is, the lower $X_{\nu p}$ is, therefore providing a lower resonant frequency. To make ν as small as possible, β must be large and hence for the lowest resonant frequency $\beta = 2\pi$. Therefore, when both faces are metallic, a thin metallic plate between faces (I) and (II), with length equal to the radius of the resonator placed from the center, provides the lowest resonant frequency. The corresponding mode is $\mathrm{TM}_{\frac{1}{2}1\delta}$ and $X_{\frac{1}{2}1} = 1.166$. When one face is metallic and one face is open with $\beta = 2\pi$, the root of Bessel derivative becomes $X_{\frac{1}{4}1}$ providing further reductions in volume and resonant frequency. In practice, however, it is impossible to have both open and metallic walls at $\phi = 0$ so we can only approach this mode for β close to 2π.

D. Annular DRA

When α is greater than zero and $\beta = 2\pi$ (faces (I) and (II) not present) we form annular DRA's, also known as ring DRA's. For this geometry the z-component field inside the cavity is written as (1) for $\nu = n$, where n is an integer.

When the inner surface (III) is set to be metallic we form a cylindrical ring DRA with a metal cylinder at $r = b$ and boundary condition $E_z|_{r=b} = 0$ [11]. The corresponding characteristic equation is

$$J'_\nu(X_{\nu p})Y_\nu(\alpha X_{\nu p}) - J_\nu(\alpha X_{\nu p})Y'_\nu(X_{\nu p}) = 0 \quad (6)$$

and typical values for the solution of $X_{\nu p}$ are listed in Table II (integer values of ν are valid). Note that as α gets larger $X_{\nu p}$ increases and, therefore, the resonant frequency increases. For small values of α, say $\alpha = 0.05$ (when α is smaller than 0.05 the DRA will be difficult to construct with a 50-Ω match) the Bessel root $X_{\nu p} = 0.930$ for mode $\mathrm{TM}_{01\delta}$.

When the inner surface (III) is set to be open we form a ring DRA and we model the inner free-space circular region $(0 \le r \le b)$ using an eigenfunction expansion as

$$E_z = FI_\nu(k_{0r}r)[C\sin(\nu\phi) + D\cos(\nu\phi)]\cos(k_z z) \quad (7)$$

where F is an arbitrary constant, I_ν is the νth-order modified Bessel function of the first kind. The wavenumber k_{0r} is given

from (2) [12], [13] as

$$k_{0r}^2 = k_z^2 - \left(\frac{2\pi f}{c}\right)^2 = k_z^2 - \frac{k_z^2 + k_r^2}{\epsilon_r}. \tag{8}$$

Matching (7) with expansion (1) across the boundary $r = b$ and assuming a perfect magnetic wall around the outer circular surface at $r = a$, we obtain the following characteristic equation:

$$\begin{aligned} k_{0r}a\, I_\nu'(\alpha k_{0r}a)&[J_\nu(\alpha X_{\nu p})Y_\nu'(X_{\nu p}) - J_\nu'(X_{\nu p})Y_\nu(\alpha X_{\nu p})] \\ &- X_{\nu p} I_\nu(\alpha k_{0r}a) \\ &\cdot [J_\nu'(\alpha X_{\nu p})Y_\nu'(X_{\nu p}) - J_\nu'(X_{\nu p})Y_\nu'(\alpha X_{\nu p})] = 0. \end{aligned} \tag{9}$$

For $\nu = n$, $\epsilon_r = 12$, optimized a/d ratio (see Section III-A), and $m = 0$ some typical values of $X_{\nu p}$ are listed in Table I in which integer values of ν and $\alpha > 0$ are for this cavity. We again note that as α increases $X_{\nu p}$ increases and, therefore, the resonant frequency increases.

E. Annular Sector DRA

Annular sector DRA's are formed when $\beta < 2\pi$ and $\alpha > 0$. The field inside the annular sector DRA takes the most general form as written in (1). The feasible modes are determined by the value of β, and the boundary conditions imposed on faces (I) and (II) in the same way as described in Section II-C. Using this analysis the exact value of the mode parameter ν may be calculated using (4) or (5) and utilizing the appropriate characteristic equation (6) or (9) (surface (III) being metallic or open) we determine $X_{\nu p}$ and calculate the resonant frequency from (2). Particular values of $X_{\nu p}$ can be found in Table I or II.

For example, consider an annular sector with α=0.1, β=π with surfaces (I), (II), and (III) being metallic. From (4) we find ν=n and select characteristic equation (6) whose solutions are given in Table II for α=0.1 and nonzero integer values of ν. The lowest resonant frequency possible is due to mode $\mathrm{TM}_{11\delta}$ (n must be nonzero) and corresponds to the root X_{11} from which we can calculate the resonant frequency by (2).

III. Compact DRA Designs

Using the results in Section II we wish to determine DRA designs that are most compact in some sense for a given mode or resonant frequency $f_{\nu pm}$. Here we define compact as having minimum volume or minimum profile.

A. Minimum-Volume DRA's

The volume of the DRA designs we have considered can be written as

$$V = \pi a^2 d\left(1 - \alpha^2\right)\frac{\beta}{2\pi} \tag{10}$$

subject to the conditions imposed by (2). A necessary condition for a minimum in the volume is when the derivatives of V with respect to the independent variables a, d, α, and β are zero.

For a given mode $X_{\nu p}$, α and β are intricately related by (3), (6), or (9) and, therefore, we restrict the minimization to when α and β are fixed leaving the two free variables a and d. We eliminate d using the constraint (2) and solve $\frac{\partial V}{\partial a} = 0$ to get the value of a for minimum volume as

$$a_{\mathrm{opt}} = \sqrt{\frac{3}{2}}\frac{\xi X_{\nu p}}{f_{\nu pm}} = \sqrt{\frac{3}{8\epsilon_r}}\frac{cX_{\nu p}}{\pi f_{\nu pm}}. \tag{11}$$

The corresponding value of d can be determined from (2) as

$$d_{\mathrm{opt}} = \sqrt{\frac{3}{\epsilon_r}}\frac{(2m+1)c}{4f_{\nu pm}}. \tag{12}$$

Equations (11) and (12) provide the minimum volume for a particular α, β and mode $\mathrm{TM}_{\nu pm+\delta}$ and to deduce the global minimum we need to consider the effect of α, β, and $X_{\nu p}$ on (10) and (11). For a particular $X_{\nu p}$ (or mode) we can deduce from (5) that when face (I) is metallic and face (II) is open we achieve the smallest β and hence a minimum in volume. Additionally, from Tables I and II we note the entries with $\alpha = 0$ have the lowest $X_{\nu p}$, providing a minimum for a, from (11). Combining this geometry configuration with the optimized a and d from (11) and (12) provides us with potential global minimum designs and these are listed in Table III for various modes at $f = 1.80$ GHz and $\epsilon_r = 12$. Because d_{opt} is independent of $X_{\nu p}$, it is constant for a particular frequency.

TABLE III
Optimal Values of a and d at 1.80 GHz, $\epsilon_r = 12$, $\alpha = 0$, $m = 0$ with One Sector Face Metallic and One Open

mode	$X_{\nu p}$	a (mm)	d (mm)	β	a/d	volume (cm^3)	
$\mathrm{TM}_{21\delta}$	3.054	28.6	20.8	45°	1.375	6.711	
$\mathrm{TM}_{11\delta}$	1.841	17.3	20.8	90°	0.829	4.878	
$\mathrm{TM}_{\frac{2}{3}1\delta}$	1.401	13.1	20.8	135°	0.631	4.205	
$\mathrm{TM}_{\frac{1}{2}1\delta}$	1.166	10.9	20.8	180°	0.525	3.913	
$\mathrm{TM}_{\frac{1}{3}1\delta}$	0.910	8.5	20.8	270°	0.410	3.575	
$\mathrm{TM}_{\frac{1}{4}1\delta}$	0.769	7.2	20.8	360°	0.346	3.404	

B. Minimum-Profile DRA's

We are also interested in designs that have the lowest profile for a particular resonant frequency. For low-profile applications [14], [15], the ratio a/d is much larger than unity and we can observe from (2) that the term $\frac{\pi a}{2d}(2m+1)$ will dominate $X_{\nu p}$ for small values of ν and p. In this situation the resonant frequency (2) will approach the limit

$$f_m = \frac{c(2m+1)}{4d\sqrt{\epsilon_r}} \tag{13}$$

implying that d does not depend on the radius a [16]. We can therefore conclude that this is a lower bound to the height d of the DRA for a given resonant frequency and material. For 1.8 GHz, $\epsilon_r = 12$, $m = 0$ the lower bound on d is 12 mm. However, even with a a/d ratio of say 3, the volume is very large at 49 cm^3.

TABLE IV
PERFORMANCE OF VARIOUS CIRCULAR SECTOR DRA'S AND AN ANNULAR DRA, $a = d = 18$ mm, AS DESCRIBED IN THE TEXT. THE BANDWIDTH OF THE DRA IS DEFINED AS VSWR ≤ 2

			Faces†		Theory		FDTD		γ	Experiment	
	α	β	(I)	(II)	f(GHz)	Mode	f(GHz)	BW	(GHz cm^3)	f(GHz)	B.W.#
1	0	360°	*n.a.*		1.85	$TM_{11\delta}$	1.90	7.6%	34.8	2.04	6.6%
2	0	360°	*n.a.*		2.63	$TM_{21\delta}$	2.80‡	2.1%	51.2	not measured	
3	0.2	360°	*n.a.*		1.86	$TM_{11\delta}$	1.95	8.4%	33.4	2.08	7.7%
4	0	360°	M	M	1.50	$TM_{\frac{1}{2}1\delta}$	1.41	2.7%	25.8	1.46	2.1%
5	0	270°	M	M	1.61	$TM_{\frac{2}{3}1\delta}$	1.54	4.9%	21.2	1.60	3.8%
6	0	180°	M	M	1.85	$TM_{11\delta}$	1.79	6.1%	16.4	1.88	6.4%
7	0	90°	M	M	2.63	$TM_{21\delta}$	2.63	13.1%	12.2	2.78	10.3%
8	0	360°	O	O	1.50	$TM_{\frac{1}{2}1\delta}$	*n.a.*		*n.a.*	*n.a.*	
9	0	270°	O	O	1.61	$TM_{\frac{2}{3}1\delta}$	2.05	8.3%	28.2	2.15	9.8%
10	0	180°	O	O	1.85	$TM_{11\delta}$	2.23	10.6%	20.5	2.39	9.4%
11	0	90°	O	O	2.63	$TM_{21\delta}$	2.90	7.3%	13.3	3.05	8.0%
12	0	360°	M	O	1.34	$TM_{\frac{1}{4}1\delta}$	*n.a.*		*n.a.*	*n.a.*	
13	0	270°	M	O	1.39	$TM_{\frac{1}{3}1\delta}$	1.52	3.1%	20.9	1.58	2.9%
14	0	180°	M	O	1.50	$TM_{\frac{1}{2}1\delta}$	1.63	4.6%	15.0	1.70	5.3%
15	0	90°	M	O	1.85	$TM_{11\delta}$	1.94	6.4%	9.1	1.99	6.5%

IV. SIMULATION RESULTS

We confirm the predictions of the approximate theory presented in Section II by using simulation results from FDTD with the same setup as in [6] and [17]. For the simulations we utilize DRA's with radius $a = 18$ mm, height $d = 18$ mm, $\epsilon_r = 12$, and a finite ground plane of 150×150 mm^2.

In Table IV we provide results from 15 simulations for various sector angles β and different α. For each row of the table we list the inner-to-outer radius ratio α, sector angle β, type of boundary conditions on surface (I), (II), (metallic, M and open, O), the predicted resonant frequency, modes from (2), and the corresponding resonant frequency and bandwidth from FDTD simulations. We also list a figure of merit γ which is the FDTD resonant frequency multiplied with the circular sector DRA volume (GHz·cm^3). The smaller γ is the smaller the DRA size for a given resonant frequency.

The first two entries 1 and 2 with $\beta = 2\pi$ are equivalent to the fundamental and the higher order modes of a conventional circular DRA. Theory and FDTD simulations both predict resonant frequencies close to 1.90 and 2.80 GHz. Entry 3 is an annular DRA with a small inner-to-outer radius ratio. Cavity theory and simulation are again accurate within about 5%. For table entries 4–7, in which both faces (I) and (II) are metallic, good agreement between the theory and simulations is obtained and the percentage error is not larger than 6%. Reductions in both volume and resonant frequency are achieved as evidenced by a smaller γ. For entries 8–11, larger variations between theory and simulations occur indicating the assumption of a perfect magnetic wall of the faces is not accurate. Entry 8 does not have any simulation results since, in practice, it is not possible to construct this geometry. The final four entries are formed when one face is a metallic while the other is open. Again simulation results for entry 12 are not included since it is impossible to construct.

One of the more significant circular sector DRA's designs is in entry 15, as it maintains the same mode, frequency and bandwidth as that for entry 1, but only taking up 25% of the volume. For resonance of DCS1800 mobile telephone bands an antenna of approximately $2\times2\times2$ cm^3 would be achievable making it a possible candidate for usage.

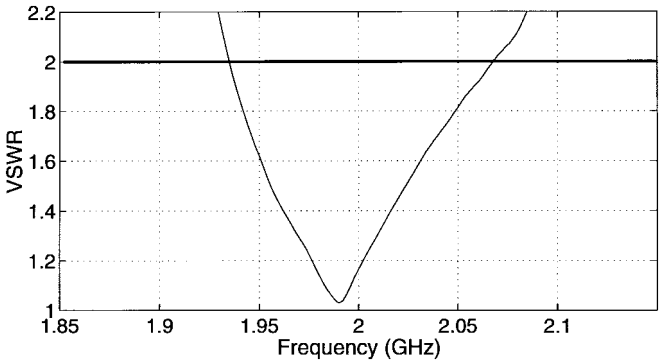

Fig. 2. VSWR (50-Ω) measurement results for the 90° circular sector DRA listed as entry 15 in Table IV.

V. EXPERIMENTAL RESULTS

We have also obtained experimental results for most of the geometries in Table IV. The circular sector DRA's are constructed by machining "ECCOSTOCK HiK" dielectric rod with $\epsilon_r = 12$ manufactured by Emerson and Cuming Inc. The measurements were made using an HP8753D network analyzer.

Good agreement with frequency and bandwidth among the theory, simulation, and measurement for the entries 4–7 are obtained while both of their sector faces are utilizing metallic plates. For entries 9–11, 13–15 the measurements agree well with their simulations for both frequency and bandwidth. A plot of the VSWR measurement for entry 15 is provided in Fig. 2. In general, FDTD simulations predict smaller resonant frequencies than actual measurements but differences are generally less than 10%. In addition, simulation and experimental results in entry 6 agree with the findings in [17].

In limited experiments we have found that sectored DRA's generally have different far-field patterns compared to conventional circular DRA operating with the same mode. For example, a sectored DRA with $\beta = \pi$ operating in mode $TM_{21\delta}$ has a main lobe in the boresight z-axis direction while for a conventional circular DRA operating in the same mode there is a null in the boresight direction.

VI. PROPOSED PCS ANTENNA DESIGN

Using the analysis and results presented in previous sections, a compact circular sector DRA is proposed for mobile handsets for DCS1800 systems. From the specifications [18], the uplink and downlink include two bands, 1710–1785 MHz and 1805–1880 MHz. A single-band antenna designed for this system should therefore work at center frequency 1795 MHz and bandwidth 170 MHz or 9.5%.

To find the most compact DRA in terms of volume and profile we use results from Section III and Table III. If we

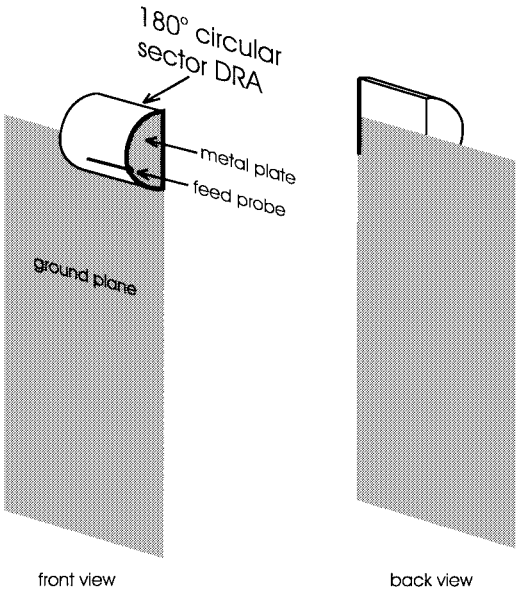

Fig. 3. Proposed 180° circular sector DRA design with $a = 12$ mm, $d = 22$ mm mounted on a $100\times$ 40 mm^2 ground plane.

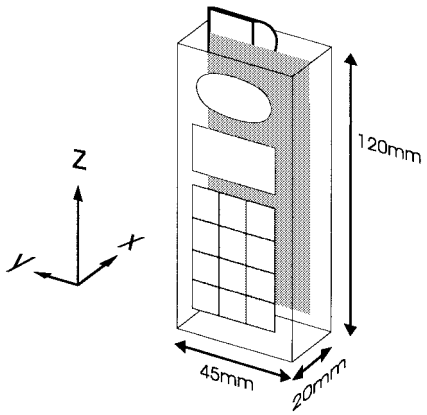

Fig. 4. Illustration of the proposed circular sector DRA integrated into a mobile telephone handset.

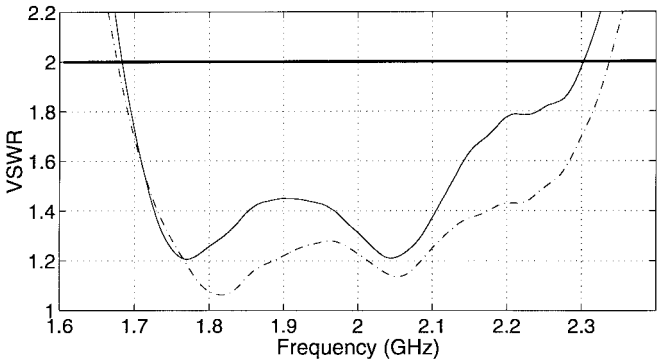

Fig. 5. Experimental VSWR results of the circular sector DRA shown in Fig. 3. Broken line is the measurement taken with a hand around the ground plane. Solid line is without hand.

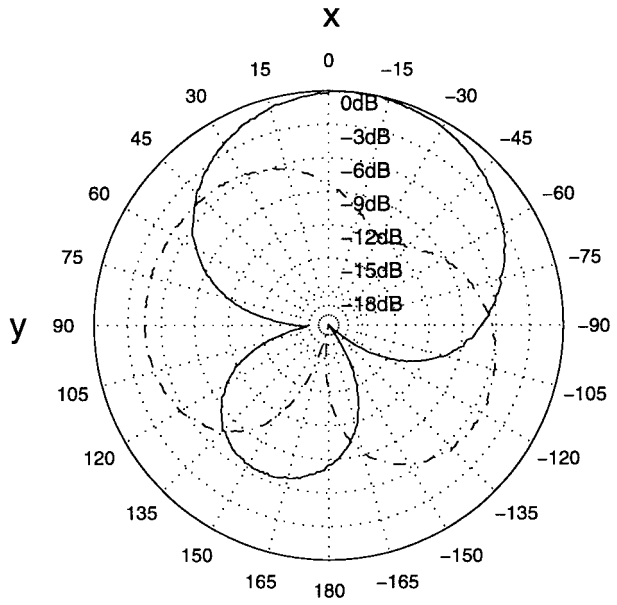

Fig. 6. Experimental far-field results of the circular sector DRA shown in Figs. 3 and 4 at 1.80 GHz in x–y plane. Solid line represents horizontal polarization and broken line, vertical polarization.

select the smallest volume we arrive at the geometry in the final entry of Table III, however, this has a high profile of $d =$ 20.8 mm. If we select the lowest profile possible (Section III-B) $d = 12$ mm the overall volume is roughly 14 times the minimum-volume geometry and is also unsuitable.

To arrive at a compromise, we have selected the forth entry in Table III and re-oriented it so the metallic plate for face (II) becomes the ground plane as shown in Fig. 3. The profile is only 10.9 mm while the volume is only 15% larger then the most compact form. In addition, this form is naturally suitable for handset design since the ground plane forms part of the circuit board of the telephone and, therefore. the antenna can be integrated into the handset as shown in Fig. 4.

Since the approximate theory generally predicts smaller resonant frequencies compared to the experiments (see Table IV), the actual dimensions of the antenna design is adjusted to $a =$ 12 mm and $d = 22$ mm. The VSWR measurement of this antenna is shown in Fig. 5 with and without a hand around the ground plane. With VSWR <2, the impedance bandwidth is from 1.68 to 2.30 GHz, while VSWR <1.5 it is from 1.71 to 2.12 GHz. This bandwidth easily satisfies the DCS1800 system specifications mentioned earlier. In fact, the bandwidth could be reduced and this could be performed by increasing ϵ_r and, therefore, reducing the DRA's overall size further.

Horizontal x–y plane far-field measurement at 1.80 GHz is presented in Fig. 6 in which E_ϕ is in solid line and E_θ in broken line. E_ϕ radiation is directed toward the back of the handset and E_θ is mainly at two sides. This indicates that radiation toward the head area should be reduced.

VII. Conclusion

We have investigated using theory, simulations, and experiments, various circular sector and annular sector DRA's. A circular sector DRA design with sector angle 90°, one metallic, and one open sector face provides the largest volume reduction for a given resonant frequency. It occupies 75% less volume than a conventional cylindrical DRA. Volume minimization for compact sector DRA design at different operating modes is also discussed. Using this result, a compact

(in both volume and profile) 180° circular sector DRA with $a = 12$ mm, $d = 22$ mm is designed and proposed for a mobile telephone handset. Experiments reveal the impedance bandwidth is 1.68–2.30 GHz (VSWR <2) easily meeting the DCS1800 system specifications and radiation is reduced toward the head area.

REFERENCES

[1] S. A. Long, M. W. McAllister, and L. C. Shen, "The resonant cylindrical dielectric cavity antenna," *IEEE Trans. Antennas Propagat.*, vol. AP-31, no. 3, pp. 406–412, 1983.

[2] R. K. Mongia and P. Bhartia, "Dielectric resonator antennas—A review and general design relations for resonant frequency and bandwidth," *Int. J. Microwave Millimeter-Wave Computer-Aided Eng.*, vol. 4, no. 3, pp. 230–247, 1994.

[3] K. M. Luk, K. W. Leung, and S. M. Shum, "Analysis of dielectric resonator amtennas," in *Advances in Microstrip and Printed Antennas*, H. K. Lee and W. Chen, Eds. New York: Wiley, 1997.

[4] A. A. Kishk, A. Ittipiboon, Y. M. M. Antar, and M. Cuhaci, "Slot excitation of the dielectric disk radiator," *IEEE Trans. Antennas Propagat.*, vol. 43, pp. 198–201, Feb. 1995.

[5] R. K. Mongia and A. Ittipiboon, "Theoretical and experimental investigations on rectangular dielectric resonator antennas," *IEEE Trans. Antennas Propagat.*, vol. 45, no. 9, pp. 1348–1356, 1997.

[6] C. R. Rowell and R. D. Murch, "A capacitively loaded PIFA for compact mobile telephone handsets," *IEEE Trans. Antennas Propagat.*, vol. 45, pp. 837–842, May 1997.

[7] C. R. Rowell and R. D. Murch, "A compact PIFA suitable for dual frequency 900/1800 MHz operation," *IEEE Trans. Antennas Propagat.*, vol. 46, pp. 596–598, Mar. 1998.

[8] G. F. Pederson and J. B. Andersen, "Integrated antennas for hand-held telephones with low absorption," in *1994 IEEE 44th Vehicular Technology Conf.*, 1994, vol. 3, pp. 1537–1541.

[9] M. A. Jensen and Y. Rahmat-Samii, "Performance analysis of antennas for hand-held transceivers using FDTD," *IEEE Trans. Antennas Propagat.*, vol. 42, pp. 1106–1113, Aug. 1994.

[10] W. F. Richards, J. D. Ou, and S. A. Long, "A theoretical and experimental investigation of annular, annular sector, and circular sector microstrip antennas," *IEEE Trans. Antennas Propagat.*, vol. AP-32, pp. 864–867, Aug. 1984.

[11] R. K. Mongia, "Small electric monopole mode dielectric resonator antenna," *Electron. Lett.*, vol. 32, no. 11, pp. 947–949, 1996.

[12] D. Kajfez and P. Guillon, Eds., *Dielectric Resonators*. Norwood, MA: Artech House, 1986.

[13] S.-W. Chen and K. A. Zaki, "Dielectric ring resonators loaded in waveguide and on substrate," *IEEE Trans. Microwave Theory Tech.*, vol. 39, pp. 2069–2076, Dec. 1991.

[14] K. P. Esselle, "A low-profile rectangular dielectric-resonator antenna," *IEEE Trans. Antennas Propagat.*, vol. 44, pp. 1296–1297, Sept. 1996.

[15] ———, "Circularly polarized higher-order rectangular dielectric-resonator antenna," *Electron. Lett.*, vol. 32, no. 3, pp. 150–151, 1996.

[16] K. W. Leung and K. M. Luk, "Circular dielectric antenna of high dielectric constant for low profile applications," in *9th Int. Conf. Antennas and Propagation*, 1995, vol. 1, pp. 517–519.

[17] M. T. K. Tam and R. D. Murch, "Half volume dielectric resonator antenna designs," *Electron. Lett.*, vol. 33, no. 23, pp. 1914–1916, 1997.

[18] M. Mouly and M. B. Pautet, "The GSM system for mobile communications," *France*, p. 217, 1992.

Matthew T. K. Tam was born in Hong Kong in 1973. He received the B.S. degree in physics (first class honors) from Hong Kong Baptist University in 1995 and the M.Phil. degree in electrical and electronic engineering from the Hong Kong University of Science and Technology in 1998.

He is currently working as a technical officer at the Centre for Wireless Information Technology, Hong Kong University of Science and Technology, and is part of a team responsible for developing a multimedia wireless communication system. His research interests include compact, multiband, diversity, and circularly polarized antennas for mobile handsets.

Ross D. Murch (S'85–M'87–SM'98) received the Ph.D. degree in electrical and electronic engineering from the University of Canterbury, Christchurch, New Zealand, in 1990 for research involving electromagnetic inverse scattering.

From 1990 to 1992 he was a Post-Doctorate Fellow at the Department of Mathematics and Computer Science at Dundee University, Scotland, where he worked on approximate approaches to electromagnetic scattering from three-dimensional objects. Currently he is an Associate Professor in the Department of Electrical and Electronic Engineering at the Hong Kong University of Science and Technology. His most recent research activities center around the application of electromagnetics and signal processing to wireless communications. Research interests include: antenna design for mobile telephone handsets, smart antenna algorithms, and propagation prediction for wireless communications. He is also the founding Director of the Center for Wireless Information Technology, which was begun in August 1997. From August to December 1998 he was on sabbatical leave at Allgon Mobile Communications, Sweden (manufactures approximately one million handset antennas per week) and AT&T Research Labs, Newman Springs Laboratory, NJ. Since 1994 he has also acted as a consultant for various industrial projects on wireless communications and has two U.S. patents related to wireless communication.

Dr. Murch acts as a reviewer for several IEEE journals and has also been involved in the organization of several international conferences and sessions. He is a Chartered Engineer, a member of IEE, and also an URSI correspondant. He received an URSI young scientist award in 1963 and an engineering teaching excellence appreciation award in 1966.